Lightweight Mesh-Based Tunnel Geometry Modeling and LiDAR Sensor Simulation for Infrastructure Monitoring

Jiangyuan SONG and Corinna HARMENING, Germany

Key words: mobile laser scanning, tunnel modeling, sensor simulation, robotics

SUMMARY

Tunnels are critical infrastructures that require efficient geometry-aware monitoring for building and maintenance. This study presents a lightweight pipeline for tunnel surface modeling and sensor simulation based on mobile laser scanning (MLS) data. Total station control points are used to constrain and correct the MLS trajectory. After filtering and segmentation, a triangular mesh of the tunnel lining is reconstructed as a compact geometric representation. Based on mesh-based ray casting, we simulate point cloud acquisition for different ranging sensors, including a terrestrial laser scanner and a low-cost LiDAR. The proposed framework supports comparison of sensor coverage and sampling characteristics in a virtual environment and provides a foundation for developing a mobile platform for digital twin monitoring in Gazebo. The methodology is demonstrated on a real tunnel dataset captured at the entrance tunnel of the Black Forest Observatory.

Lightweight Mesh-Based Tunnel Geometry Modeling and LiDAR Sensor Simulation for Infrastructure Monitoring

Jiangyuan SONG and Corinna HARMENING, Germany

1. INTRODUCTION

Tunnels are critical infrastructures used in transportation, construction, and utilities. Their safe operation depends on continuous monitoring of structural conditions (Strauss et al., 2020). Compared with open environments, tunnel monitoring is constrained by limited accessibility, safety requirements, and challenging sensing conditions. These constraints increase the demand for an efficient design of the tunnel monitoring system and the operation process. With the development of digital twin technology, tunnel monitoring can be virtually simulated, reducing design costs and enabling more comprehensive solutions. This study developed a high-fidelity 3D model with tunnel geometry reconstruction and laser scanner simulation for tunnel monitoring, which is a prerequisite for achieving a digital twin tunnel.

Geometric tunnel models are a cornerstone of the tunnel simulation. The quality and completeness of the geometric model directly affect the reliability of downstream tasks. However, acquiring tunnel geometry remains difficult. Many tunnels lack accurate design drawings or up-to-date building information models (BIM), particularly for older infrastructure or natural tunnels. Traditional total station surveys offer high-accuracy control and are widely used for deformation monitoring. However, the measurement points are typically sparse and cannot capture complex surface details. Terrestrial laser scanning can produce dense and accurate point clouds, but it requires multiple scan stations, is sensitive to occlusions and often has data gaps, especially in narrow tunnel environments. Mobile Laser Scanning (MLS) can offer efficient continuous acquisition and can improve coverage by continuous scanning through the tunnel.

In addition to modeling, sensor simulation has become an important tool for reducing cost and risk in monitoring tasks. Before starting field campaigns, engineers often need to decide sensor type, configuration, and acquisition strategy (station locations or trajectories) for the monitoring requirements. Performing such comparisons purely through field trials is expensive and time-consuming. A realistic tunnel model combined with sensing simulation can enable early evaluation of sensor configurations and guide acquisition planning and equipment selection.

A tunnel scenario at the entrance tunnel of the Black Forest Observatory (BFO) (Germany) is studied in this work, as shown in Figure 1. The investigated section is approximately 300 m long and represents an elongated geometry and limited accessibility. This study presents a lightweight framework integrating drift-corrected MLS tunnel modeling with mesh-based laser raycasting simulation to support monitoring-oriented workflows. The methodology first employs total station control points to constrain and rectify the inherent drift in MLS data,

followed by robust filtering and segmentation techniques to isolate the tunnel lining from ambient noise. To facilitate geometric queries and physics-based interactions, the processed point cloud is reconstructed into a triangular mesh representation. With this mesh environment, the framework utilizes ray-casting algorithms to simulate the range measurements of diverse laser sensors, enabling a comparative analysis of sensor-specific point clouds regarding spatial coverage, sampling patterns, and potential data occlusions. Furthermore, the resulting tunnel mesh can be integrated into the Gazebo simulation to provide a realistic simulation environment for robot motion and sensing. This enables the development of digital twins for robotic mobile platforms and structural health monitoring systems.

Figure 1: ZF 5016 Flexscan MLS system and BFO environment.

The remaining part of the paper proceeds as follows: Section 2 reviews related work in tunnel survey and sensor simulation. Section 3 presents the mesh-based ray casting methodology and sensor models. Section 4 evaluates simulated sensing results and discusses monitoring and robotics applications. Section 5 concludes and outlines future extensions, including richer environmental effects and more realistic sensor response modeling.

2. RELATED WORK

2.1 3D Tunnel Survey

The development of laser scanning technology enables 3D point cloud data acquisition for tunnel surveying. Unlike the total station survey, 3D laser scanning technology captures millions of points, enabling the precise reproduction of surface details (Strauss et al., 2020). However, the characteristic of TLS needs multiple scan stations to avoid occlusions in elongated tunnel environments, leading to significant time consumption and registration complexities (Cabo et al., 2017). MLS offers a more efficient alternative by enabling continuous acquisition from moving platforms (Chrbolková et al., 2025).

The primary challenge in subterranean MLS is the SLAM drift. Unlike open environments, tunnels lack Global Navigation Satellite System (GNSS) signals. To avoid the LiDAR SLAM drift, wheel odometry and the inertial measurement unit (IMU) are commonly selected to provide another source of the trajectory (Liu et al., 2025). However, the above solutions all have inherent drifts. Therefore, in this study, we combined a control point network composed of traditional total stations and prisms with MLS, using the control network to correct the SLAM drift of the MLS.

2.2 Digital Twins for Tunnel Monitoring

Digital twin is becoming an important technology for the lifecycle management of civil infrastructure. Compared with a static BIM, a digital twin functions as a dynamic virtual replica that maintains real-time data integration and bidirectional exchange with its physical counterpart (Pan et al., 2021). Recent implementations visualize structural anomalies directly on 3D meshes, such as water ingress (Huang et al., 2020). With trained machine learning models, digital twins can support predictive maintenance and utilize extended reality (XR) technologies for maintenance operations (Coupry et al., 2021). Structural failures can also be predicted through the simulation of digital twins and machine learning models (Liu et al., 2024). In this study, the simulation environment focuses on the virtual replication of laser sensors within a tunnel model and the extension for robotic platforms, serving as a basis for a future digital twin.

2.3 Sensor Simulation

Sensor simulation is a component of monitoring-oriented digital twins, which enables the early evaluation of equipment configurations and acquisition strategies. The core of laser sensor simulation is the ray-casting or ray-tracing algorithms. These algorithms define a virtual ray by its origin and scan direction, calculating the intersection with a 3D environmental model to generate synthetic point clouds (Winiwarter et al., 2022). The fidelity of these synthetic point clouds is dependent on the environmental model. Triangular meshes are one of the preferred formats for high-fidelity simulations due to their ability to provide continuous surfaces and simplify complex physics-based interactions, such as ray-triangle intersection (Möller et al., 2005). Complex simulators such as LiMOX enable real-time simulation of pulsed lidar interactions by integrating material databases to account for reflectivity and incident angle effects (Rott et al., 2024).

Beyond specialized LiDAR or laser scanner simulators, multifunctional simulators have been broadly employed to accelerate the development of perception systems, particularly in recent years of autonomous driving development. For example, CARLA, an open-source simulator built on the Unreal Engine, provides photorealistic environments for testing autonomous perception algorithms under diverse traffic and weather conditions (Dosovitskiy et al., 2017). Similarly, AirSim offers a cross-platform simulation environment for drones and ground vehicles (Shah et al., 2017). For robotics research, Gazebo stands as the industry standard due to its robust support for multiple high-performance physics engines and seamless integration with the Robot Operating System (ROS) (Koenig and Howard, 2004). These platforms allow

for the generation of large-scale synthetic datasets, which are crucial for training deep learning models.

The LiDAR simulator described in the following part of this study is a lightweight distance simulator. By utilizing ray tracing algorithms from Open3D and a custom sensor model, LiDAR simulation can be achieved with just a few lines of code. Furthermore, both the sensor model and environment model are based on real-world measurements, making them more realistic for our specific scenarios in BFO.

3. LASER SIMULATION METHODOLOGY

3.1 Data Acquisition and Pre-Processing

The dataset was collected in the entrance tunnel of the BFO, which is approximately 300 meters long. GNSS is unavailable in the tunnel, and the elongated geometry leads to SLAM drift (Song et al., 2026). MLS data were acquired on a wheeled platform with the ZF 5016 Flexscan system, as shown in Figure 1.

To constrain the MLS drift, a control network was established using a total station with prism measurements. Control points distributed along the tunnel wall provide an external reference frame and allow drift to be reduced by aligning the MLS point cloud to the surveyed reference frame in the software LaserControl from Zoller & Fröhlich GmbH.

After drift correction, point cloud pre-processing is applied to improve scan surface quality for meshing. Outliers and spurious returns are removed through manual filtering. Furthermore, voxel downsampling is applied in 2 cm for balancing the computational efficiency and geometric fidelity.

3.2 Mesh-based Environment Representation

To transform the point clouds into a continuous and queryable surface, a mesh reconstruction in CloudCompare based on Poisson Surface Reconstruction (PSR) was implemented.

First, surface normals are estimated with the triangulation surface model setting in CloudCompare. Second, the PSR algorithm is applied (Kazhdan et al., 2024). This global optimization reconstruction algorithm yields a seamless, watertight manifold that is highly stable to localized sampling non-uniformities and minor data gaps. Finally, a post-processing stage is implemented to address the PSR algorithm's tendency to generate closed surfaces, which often creates bulbous closures at the tunnel gate. The resulting high-fidelity, open-ended tunnel model is preserved in .ply format, serving as the environment model for subsequent laser sensor simulations. The resulting mesh model of the tunnel is shown in Figure 2. The color gradient visualizes the spatial distribution of point density mapped onto the mesh. Regions in red signify a strong correspondence between the reconstructed surface and the empirical sample points, whereas blue regions signify extrapolated surfaces in areas of data occlusion or low

sampling density. The blue areas are primarily located at the edges of the model and in the sections of the tunnel covered by water.

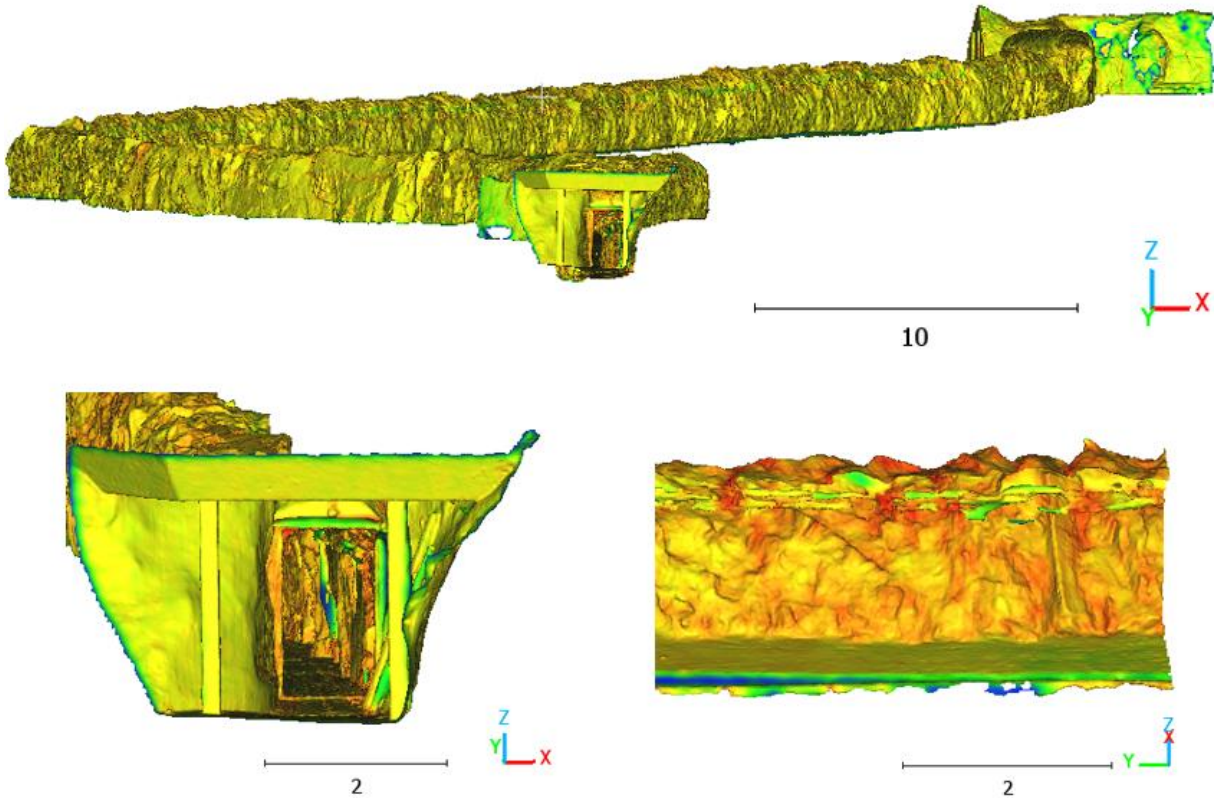

Figure 2: Reconstructed tunnel mesh model. The color gradient represents the spatial distribution of point density mapped onto the mesh surface, with the scale bar in meters.

3.3 Mesh-based Ray Casting

A mesh-based ray-casting methodology is used to emulate the data acquisition process of LiDAR sensors within the reconstructed tunnel mesh environment. This approach treats each laser pulse as a line and computes its intersection with the triangular mesh. For the core intersection logic, we utilize the Möller–Trumbore algorithm, an efficient method for computing the intersection of a ray and a triangle in 3D space (Möller et al., 2005). Unlike traditional methods that require the pre-calculation of the plane equation for each triangle, the Möller–Trumbore algorithm leverages barycentric coordinates to determine intersections directly.

As in Figure 3, a point $\hat{\mathbf{p}}$ on a triangle defined by vertices $\mathbf{p}_A$, $\mathbf{p}_B$, and $\mathbf{p}_C$ can be expressed as:

$$\hat{\mathbf{p}} = (1 - a_0 - a_1)\mathbf{p}_A + a_0\mathbf{p}_B + a_1\mathbf{p}_C,$$

where a_0 and a_1 are the barycentric coordinates. For a successful intersection, this point must also lie on the ray defined by the sensor position $\boldsymbol{x}$ and the beam orientation unit vector $\mathbf{v}$

$$\hat{\mathbf{p}} = \mathbf{x} + t\mathbf{v},$$

where t represents the distance from the sensor to the intersection point. By equating these expressions, the intersection problem is transformed into a linear system solved via Cramer's rule:

$$[-\mathbf{v} \quad (\mathbf{p}_B - \mathbf{p}_A) \quad (\mathbf{p}_C - \mathbf{p}_A)] \begin{bmatrix} t \\ a_0 \\ a_1 \end{bmatrix} = \mathbf{x} - \mathbf{p}_A.$$

An intersection is considered valid if $t > 0$.

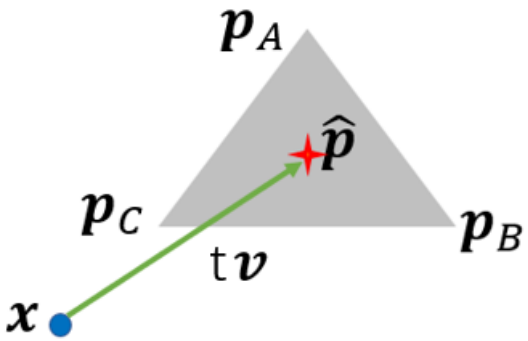

Figure 3: Müller-Trumbore Ray Casting Algorithm illustration

To ensure high computational throughput for simulating high-resolution TLS and high-frequency LiDAR, the Intel Embree ray-tracing kernel via the Open3D library is applied (Zhou et al., 2018). Spatial acceleration structures are applied to minimize the time of ray-triangle casting.

3.4 Laser Scanners Modeling

For comparing different acquisition strategies for tunnel surveying, we configured the ray-casting framework to emulate two distinct types of laser scanners: a high-precision TLS and a mobile profile scan LiDAR.

3.4.1 Terrestrial Laser Scanner Z+F IMAGER 5016

The Z+F IMAGER 5016 is a high-resolution TLS. TLS scans statically on the tripod. The scanning mechanism was simulated in spherical coordinates with a field of view (FoV) of 360° horizontally and 320° vertically, as in Figure 4, left. We employed an angular resolution of 0.016° to simulate a SUPERHIGH density acquisition setting.

3.4.2 Mobile Profile LiDAR: Robosense Airy

The Robosense Airy is a mobile robot perception LiDAR with hemispherical profile scanning mode. It has a 96-line digital scanning architecture. We simulated its 360° horizontal field of view and 90° vertical field of view (s. Figure 4, right); this wide-angle characteristic gives it excellent near-field coverage in confined spaces such as tunnels.

While the TLS model remains stationary, the Robosense Airy simulation is coupled with a time-dependent trajectory where the sensor origin **x** and orientation **v** are updated at each time step. This trajectory-based approach enables the framework to replicate the helical sampling patterns, so the simulation can mimic the rolling shutter effect. By incorporating these motion-induced distortions alongside sensor-specific uncertainties, the simulator can evaluate how vehicle speed and mounting configurations impact the MLS.

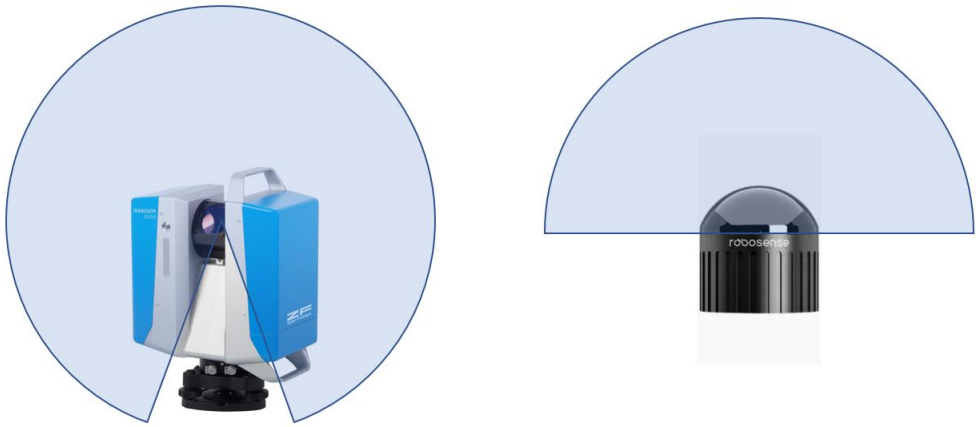

Figure 4: FoV of the Laser Scanners. Left: Z+F Imager 5016 (Zoller + Fröhlich, 2026), Right: Robosense Airy (RoboSense, 2026)

4. SIMULATION EVALUATION AND APPLICATION

4.1 Quantitative Verification of Simulated Point Clouds

The geometric fidelity of the designed simulator was validated by directly comparing individual simulated point clouds with their corresponding real-world point clouds. The point clouds in the illustrations are color-coded based on Z-axis height, as shown in Figure 5. As shown in the figure, the two point clouds generally visually match. However, in the real point cloud, there are additional artifacts arising from the measurement tripod, which can be avoided by using a simulated point cloud. However, for the cable section on the left most part, the simulated point cloud fails to represent the four separate cables due to insufficient resolution when modeling the tunnel mesh.
The uncertainty was quantified using a Cloud-to-Cloud (C2C) distance analysis, comparing the simulated points against the reference data. This evaluation was conducted across 15 TLS scan samples evenly distributed along a 300-meter tunnel with Z+F IMAGER 5016, yielding mean

distances ranging from 0.0080 m to 0.1410 m with an overall average of 0.0513 m, detailed in Table 1. The variation primarily originates from measurement uncertainties in the raw MLS data and the mesh modeling process.

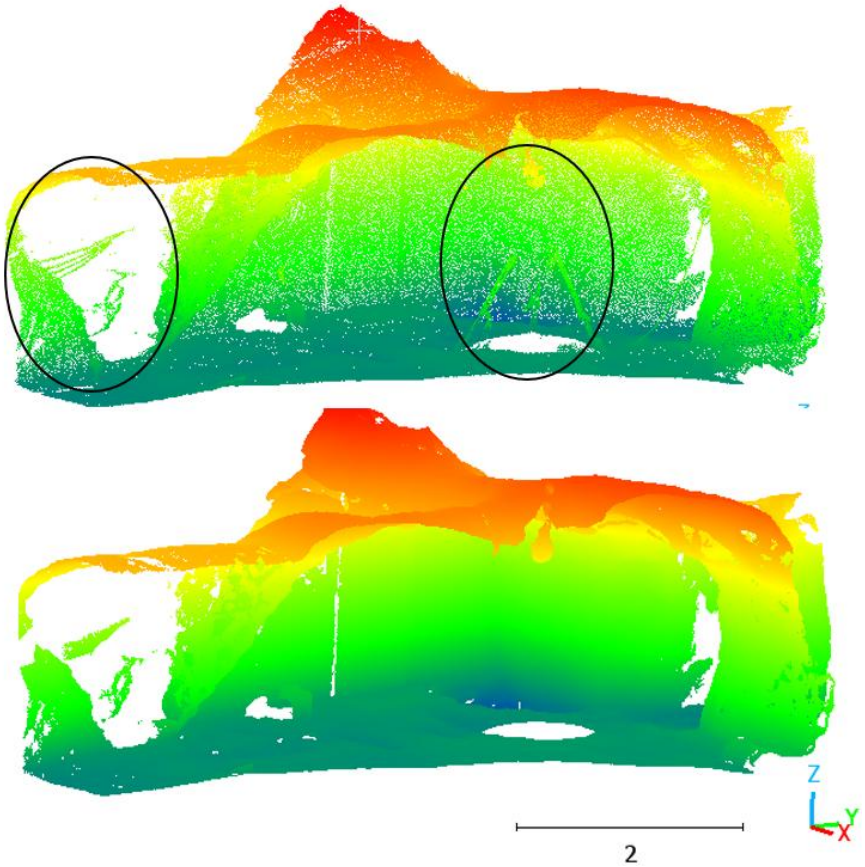

Figure 5: Comparison between the experimental Z+F IMAGER 5016 point cloud (top) and the simulated counterpart (bottom). Black circles highlight distinct regions of interest. Both point clouds are color-coded according to the Z-axis elevation.

4.2 Monitoring-Oriented Applications

4.2.1 Optimal Deployment of TLS Stations under Occlusions

This application utilizes the simulation to determine the minimum number of static TLS stations required to achieve target coverage in the narrow tunnel. To optimize the deployment plan, we evaluated the coverage efficiency at varying intervals of 5 and 10 meters station spacing (s. Figure 6). Taking the current scanning position (indicated in green) as a baseline, the simulation demonstrates that placing the subsequent station at a 5 m interval (blue) provides sufficient overlap to achieve a seamless reconstruction of the tunnel lining; however, increasing this distance to 10 m (red) results in significant data gaps where the sensor's FoV is obstructed, as .

These results provide a quantitative basis for balancing field-work duration with data completeness.

Table 1: Simulated point cloud evaluation C2C results (Z+F IMAGER 5016)

TLS scan	mean – m	median – m	std – m
1	0.087225	0.05337	0.106043
2	0.038868	0.034642	0.02621
3	0.035715	0.033457	0.021561
4	0.095164	0.117723	0.054169
5	0.140976	0.157869	0.071598
6	0.116235	0.121741	0.075281
7	0.042484	0.038199	0.027921
8	0.016884	0.011103	0.022921
9	0.052265	0.037546	0.059637
10	0.031651	0.027757	0.026696
11	0.047087	0.020347	0.068353
12	0.034213	0.014369	0.056493
13	0.014358	0.007084	0.033031
14	0.008194	0.006548	0.013826
15	0.008024	0.006543	0.010382

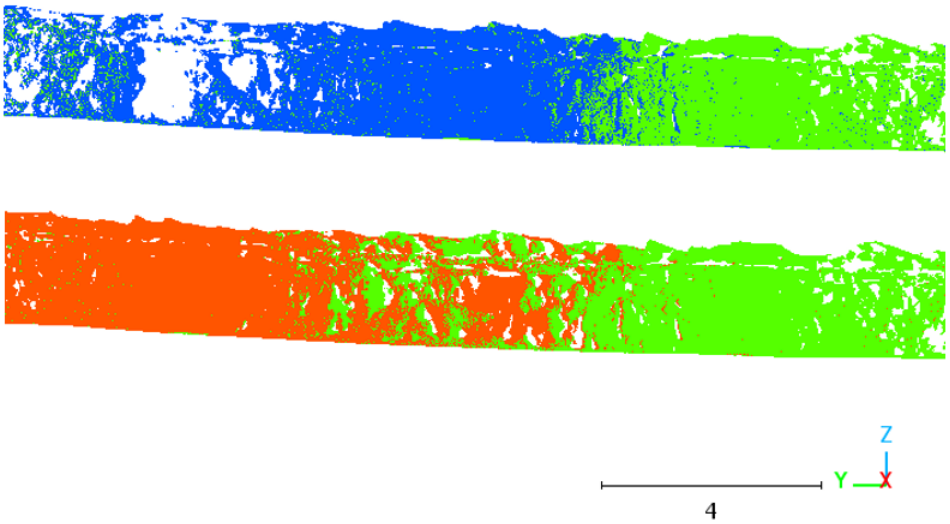

Figure 6: TLS occlusions simulation.
Current scanning position(green), 5 m interval (blue), 10 m interval (red)

4.2.2 Impact of MLS Scanning Frequency and Travel Speed

This part of the study investigates the trade-off between operational efficiency and geometric fidelity in mobile laser scanning by simulating various combinations of scanning frequencies and platform travel speeds. Utilizing the Robosense Airy model with the sensor oriented

downward along the Z-axis toward the ground, we quantify the resulting point density and the severity of the rolling shutter effect. As illustrated in Figure 7, the sensor moving speed at 0 m/s (red), 1 m/s (green), and 3 m/s (blue) reveals distinct geometric characteristics: while the static sensor generates a perfectly symmetrical pattern of concentric circles on the ground, the increase in travel speed progressively distorts these rings into a stretched configuration. This distortion shows that for high-accuracy MLS requirements and SLAM algorithms, the rolling shutter effect is a critical factor that must be compensated for to prevent structural distortion in the final point cloud.

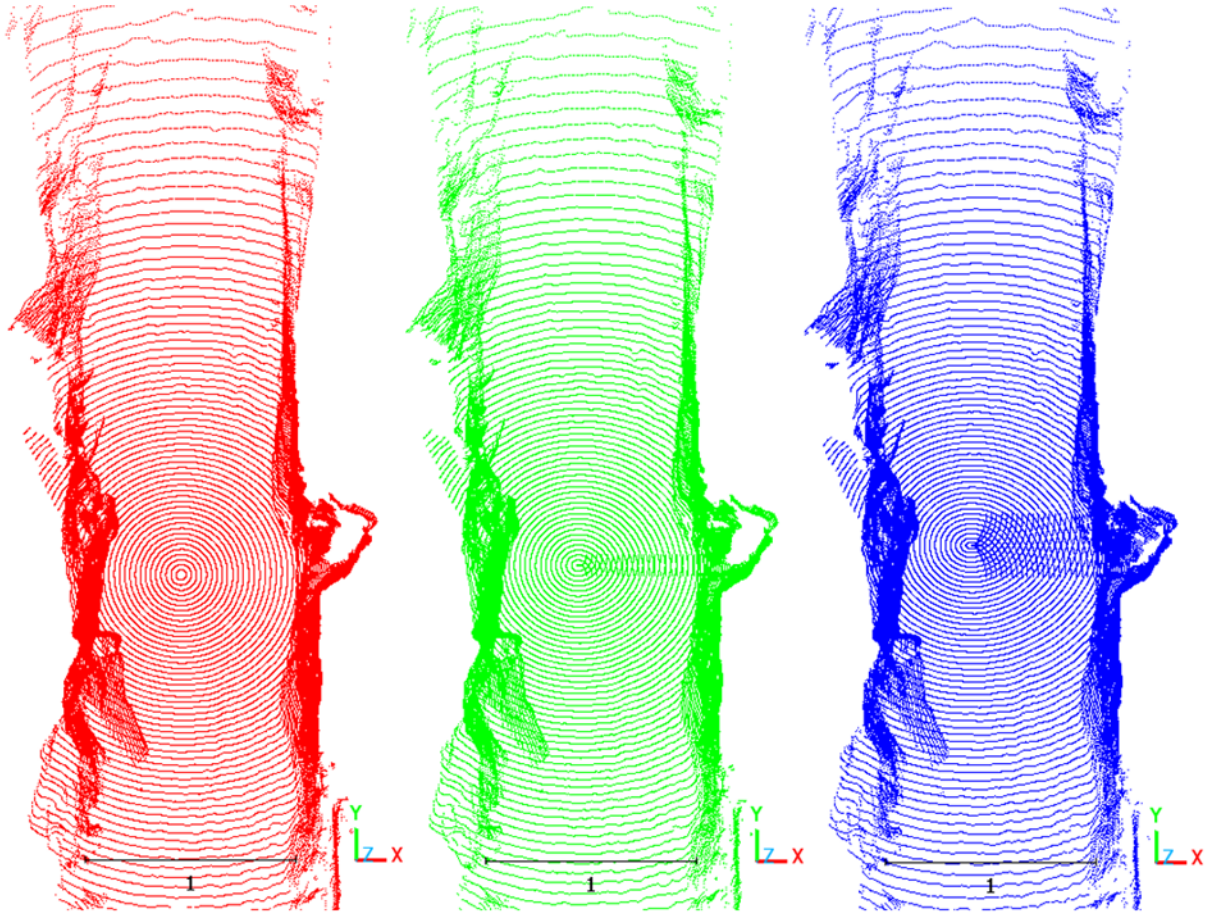

Figure 7: Rolling-shutter effect simulation.
Sensor moving speed at 0 m/s (red), 1 m/s (green), and 3 m/s (blue).

4.2.3 Integration with Robotic Platforms in Gazebo

The tunnel mesh and sensor model have been integrated into the Gazebo environment to support autonomous robot development, as demonstrated by the Agilex LIMO robot in our tunnel mesh model, as in Figure 8. By adopting ROS Robot Operating System, Gazebo provides a framework for testing navigation and sensor algorithms within a high-fidelity physics engine. The use of real environmental data ensures robots encounter real-world challenges, such as

complex occlusions and irregular geometries. It can minimize the gap between simulation and reality, enabling robots' behaviors to undergo safe, repeatable testing before field deployment, significantly reducing development costs and hardware risks.

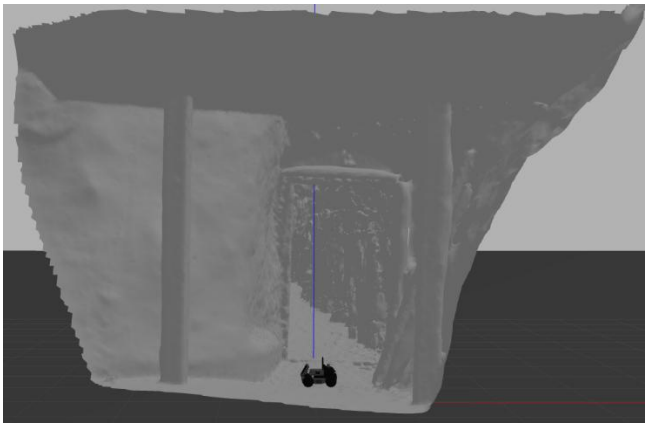

Figure 8: Tunnel mesh in Gazebo with LIMO robot.

5. CONCLUSION AND OUTLOOK

5.1 Conclusion

This study proposes a lightweight workflow for tunnel geometry modeling and sensor simulation. By integrating total station control networks with MLS, the point cloud of the BFO was effectively acquired and mitigated SLAM-related drift issues, establishing reliable data for downstream simulations. By reconstructing the survey point clouds into triangular meshes, the tunnel lining structure is represented in a format that enables efficient ray-surface intersection. The generated model supports systematic simulation of diverse ranging sensors, spanning from high-precision static terrestrial laser scanners to cost-effective mobile LiDAR systems. Furthermore, the generated mesh's compatibility with robotics simulation platforms like Gazebo bridges the gap between static structure modeling and dynamic autonomous navigation, providing a realistic environment for developing robotic monitoring platforms.

5.2 Outlook

Despite the many advantages of this lightweight framework, several areas remain available for future improvement. Current simulations primarily handle visibility issues through idealized ray casting; however, real-world sensor performance is significantly influenced by physical factors such as material reflectivity, incident angle, and beam convergence. The integration of these reflectivity measurements and physical properties would substantially enhance the realism of digital twins, particularly when comparing sensors with different wavelengths. Furthermore, including dynamic elements and environmental noise, such as dust and humidity, into models would more accurately reflect the nature of tunnel operating environments. Additionally, follow-up iterations of this research will aim to integrate multimodal

environmental data. Incorporating color, temperature, and humidity into the mesh-based model framework. This can enable optical camera simulation and can support multi-sensor fusion studies.

REFERENCES

Cabo, C., Ordóñez, C. and Argüelles-Fraga, R., 2017. An algorithm for optimizing terrestrial laser scanning in tunnels. Automation in Construction, 83, pp.163-168.

Chrbolková, A., Štroner, M., Urban, R., Michal, O., Křemen, T. and Braun, J., 2025. A Comparative Study of Indoor Accuracies Between SLAM and Static Scanners. Applied Sciences, 15(14), p.8053.

Chrbolková, A., Štroner, M., Urban, R., Michal, O., Křemen, T. and Braun, J., 2025. A Comparative Study of Indoor Accuracies Between SLAM and Static Scanners. Applied Sciences, 15(14), p.8053.

Dosovitskiy, A., Ros, G., Codevilla, F., Lopez, A. and Koltun, V., 2017, October. CARLA: An open urban driving simulator. In Conference on robot learning (pp. 1-16). PMLR.

Huang, H., Cheng, W., Zhou, M., Chen, J. and Zhao, S., 2020. Towards automated 3D inspection of water leakages in shield tunnel linings using mobile laser scanning data. Sensors, 20(22), p.6669.

Kazhdan, M., Chuang, M., Rusinkiewicz, S. and Hoppe, H., 2020, August. Poisson surface reconstruction with envelope constraints. In Computer graphics forum (Vol. 39, No. 5, pp. 173-182).

Koenig, N. and Howard, A., 2004, September. Design and use paradigms for gazebo, an open-source multi-robot simulator. In 2004 IEEE/RSJ international conference on intelligent robots and systems (IROS)(IEEE Cat. No. 04CH37566) (Vol. 3, pp. 2149-2154). Ieee.

Liu, W., Qi, Y., Guan, T. and Liang, Y., 2025. Efficient and accurate 3D reconstruction in a featureless tunnel environment: a robust LiDAR-Inertial SLAM tightly coupled with wheel odometry. Journal of Civil Structural Health Monitoring, 15(8), pp.3575-3588.

Liu, Z., Yuan, C., Sun, Z. and Cao, C., 2022. Digital twins-based impact response prediction of prestressed steel structure. Sensors, 22(4), p.1647.

Möller, T. and Trumbore, B., 2005. Fast, minimum storage ray/triangle intersection. In ACM SIGGRAPH 2005 Courses (pp. 7-es).

Pan, Y. and Zhang, L., 2021. A BIM-data mining integrated digital twin framework for advanced project management. Automation in Construction, 124, p.103564.

RoboSense, 2026, Airy - RoboSense LiDAR, https://www.robosense.ai/en/rslidar/Airy, Shenzhen, RoboSense Co., Ltd., [Accessed: January 15, 2026].

Rott, R., Ritter, D.J., Ladstätter, S., Nikolić, O. and Hennecke, M.E., 2024. LiMOX—A point cloud Lidar model toolbox based on NVIDIA OptiX ray tracing engine. Sensors, 24(6), p.1846.

Shah, S., Dey, D., Lovett, C. and Kapoor, A., 2017, November. Airsim: High-fidelity visual and physical simulation for autonomous vehicles. In Field and service robotics: Results of the 11th international conference (pp. 621-635). Cham: Springer International Publishing.

Song, J., Bayer, L., & Harmening, C., 2026. Quality-controlled 3D tunnel mapping using terrestrial and mobile laser scanning with total station integration. Contributions to International Conferences on Engineering Surveying (INGEO 2025), Brno, Czech Republic. Accepted for publication.

Strauss, A., Bien, J., Neuner, H., Harmening, C., Seywald, C., Österreicher, M., Voit, K., Pistone, E., Spyridis, P. and Bergmeister, K., 2020. Sensing and monitoring in tunnels testing and monitoring methods for the assessment of tunnels. Structural concrete, 21(4), pp.1356-1376.

Winiwarter, L., Pena, A.M.E., Weiser, H., Anders, K., Sánchez, J.M., Searle, M. and Höfle, B., 2022. Virtual laser scanning with HELIOS++: A novel take on ray tracing-based simulation of topographic full-waveform 3D laser scanning. Remote Sensing of Environment, 269, p.112772.

Zhou, Q.Y., Park, J. and Koltun, V., 2018. Open3D: A modern library for 3D data processing. arXiv preprint arXiv:1801.09847.

Zoller + Fröhlich, 2026, Z+F IMAGER® 5016, https://www.zofre.de/en/laser-scanners/3d-laser-scanner/z-f-imagerr-5016-1, Wangen im Allgäu, Zoller + Fröhlich GmbH, [Accessed: January 15, 2026].

BIOGRAPHICAL NOTES

Song Jiangyuan is a Ph.D. candidate at the Geodetic Institute, Karlsruhe Institute of Technology (KIT), Germany. His research focuses primarily on laser scanning, particularly mobile laser scanning, including sensor fusion methods, the development of low-cost laser scanning systems, and digital twin applications integrating robotic technologies.

Prof. Dr. Corinna Harmening received her PhD from TU Vienna in 2020 and is professor for geodetic sensor systems at Geodetic Institute, Karlsruhe Institute of Technology (KIT), Germany since 2022. Her research foci are on terrestrial laser scanning, particularly on point

cloud modelling and point cloud-based deformation modelling as well as on the setting up and the evaluation of geodetic sensor systems. She is active in FIG Commission 6 “Engineering Surveys” as chair of the working group 6.1 “Deformation Monitoring and Analysis”.

CONTACTS

Jiangyuan Song
Karlsruhe Institute of Technology
Englerstraße 7
76131 Karlsruhe
Germany
+49 15255848629
jiangyuan.song@kit.edu
https://www.gik.kit.edu